HiSST: 3rd International Conference on
High-Speed Vehicle Science Technology
14 -19 April 2024, Busan, Korea

Properties of Direct Current Discharge in a Supersonic Flow, and Its Application for Plasma-Assisted Combustion

Aleksandr A. Firsov[1], Roman S. Troshkin[2], Luka S. Volkov[2], Dmitriy A. Tarasov[2], Anastasia S. Dobrovolskaya[2], Valentin A. Bityurin[2], Aleksey N. Bocharov[2]

Abstract

The article presents the results of recent studies of direct current discharge in a supersonic flow and its application for plasma-assisted combustion. Properties such as the dependence of the discharge temperature on the current and the current-voltage characteristic are described, and the results of modeling a discharge in a supersonic flow in the CFD software Plasmaero and FlowVision are presented. Based on previous results and new information obtained about the discharge and the features of plasma-assisted combustion, an experiment on the ignition of gaseous fuel in a supersonic flow under conditions where the fuel is pre-mixed with air and supplied in supersonic mode to the core of a supersonic flow is proposed and tested. This formulation of the problem excludes the influence of mixing and subsonic separation zones on the result of the experiment. It is shown that, despite preliminary mixing, an elongated powerful plasma channel is required for ignition.

Keywords: *DC discharge, supersonic flow, ignition, combustion, scramjet*

1. Introduction

Various studies of the interaction between electrical discharge and a high-speed flow were performed in relation to several major problems: plasma aerodynamics/plasma flow control [1], mixing enhancement [2], and ignition / flame stabilization in a supersonic flow using discharge[3], which is one fundamental in the development of a ramjet or a scramjet engine. Among the various types of discharges, the most commonly used discharge for the latter task is a direct current discharge or an arc discharge. Various configurations of discharge are considered [2,4], as well as combinations of electric discharge and mechanical approaches, for example, combining a discharge and a cavity[5,6].

At the same time, research into the properties of direct current discharge continues: dynamics of discharge and flow structure were described for multi-filament configuration [7], discharge location in the mixing layer of carbon-contained gas jet with supersonic air flow was discussed [8], influence of electrode geometry was noted [9,10], several approaches to discharge modelling were performed [11,12], including consideration of the issue of discharge re-breakdown (or re-strike) [13,14]. This article reports on our recent research results on longitudinal and longitudinal-transverse DC discharge, and its application to ignite a fuel mixture in a supersonic flow, with the aim of further fundamental development of the concept of plasma-assisted combustion.

2. Properties of DC discharge in a supersonic airflow

A DC discharge or Q-DC discharge in a supersonic flow, if ignited in the gap which are perpendicular to the flow (or has a perpendicular component), is stretched into the form of a U-shaped loop along the flow (Fig. 1a). Repeated re-breakdowns take place in the area near the electrodes, thus maintaining the length of the plasma filament in a certain interval. Such a discharge is usually called longitudinal-transverse, because it has a current component perpendicular to the flow. Due to the periodic length changing, the discharge voltage also pulsates and the current pulsates slightly. The peculiarities of this discharge behaviour are described below.

[1] *JIHT RAS, 125412, Izhorskaya st. 13 Bd.2, Moscow, Russia, af@jiht.org*
[2] *JIHT RAS, 125412, Izhorskaya st. 13 Bd.2, Moscow, Russia*

However, longitudinal-transverse discharge, due to its non-stationary nature, is of little use for studying a number of characteristics. Therefore, in order to clarify the properties of the discharge, such as temperature, voltage-current dependency, etc., it was decided also to study a longitudinal discharge in the core of a supersonic flow, away from the channel walls. For this purpose, a special electrode system was prepared, creating a longitudinal discharge between coaxial electrodes with a distance of 30 mm between them. An additional third electrode was used to ignite the discharge.

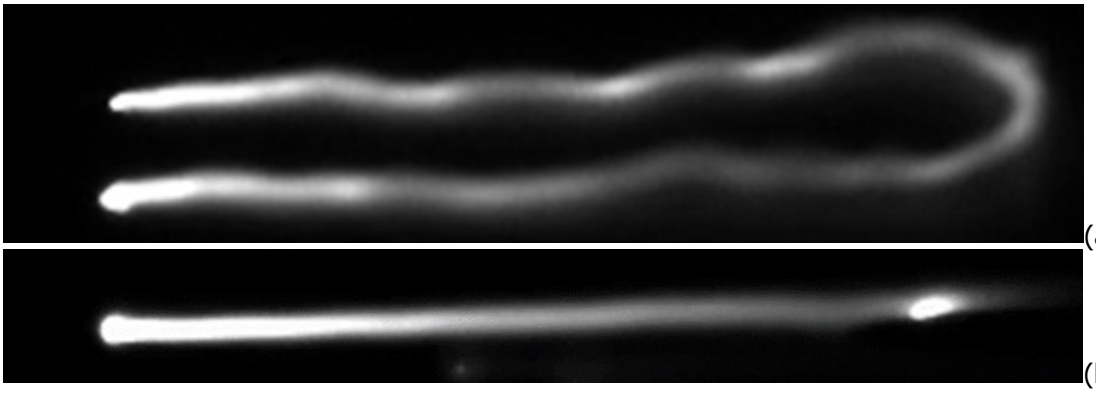

Fig 1. Longitudinal-transverse (a) and longitudinal (b) DC discharge in a supersonic flow

2.1. Longitudinal-transverse DC discharge

The peculiarities of the longitudinal-transverse discharge were studied in detail in the work[10]. Here we note the key properties, such as linear dependence of the discharge voltage on its length, and a significant decrease in the specific voltage with an increase in the discharge current (shown in Fig. 2a). It is also important to note that despite the fact that re-breakdowns do not have a specific frequency (which can be identified using Fourier analysis), statistical analysis shows that they occur at frequencies of 10-20 kHz under the considered conditions (M = 2, P = 22 kPa, T_0 = 300 K, 5-7 mm gap).

Another peculiarity is the location in which re-breakdown should occur (i.e. a new cross-flow plasma path appears, through which the discharge current begins to flow): the re-breakdowns are not located in the place where the voltage between the elements of the plasma channel is maximum (between the electrodes), but downstream by 10-30 mm. Preliminary experiments and calculations showed that this peculiarity takes place due to the fact that the process of producing electrons in the gap does not occur instantly and takes some time, which, under supersonic flow conditions, leads to the mentioned displacement downstream from the electrodes. Numerical simulation of the discharge, taking into account the breakdown, was studied in [13,15] in a 2D formulation using the Plasmaero software package (the calculation result is shown in Fig. 2b) and in [16] in 3D formulation in FlowVision software to clarify the properties and features of the discharge.

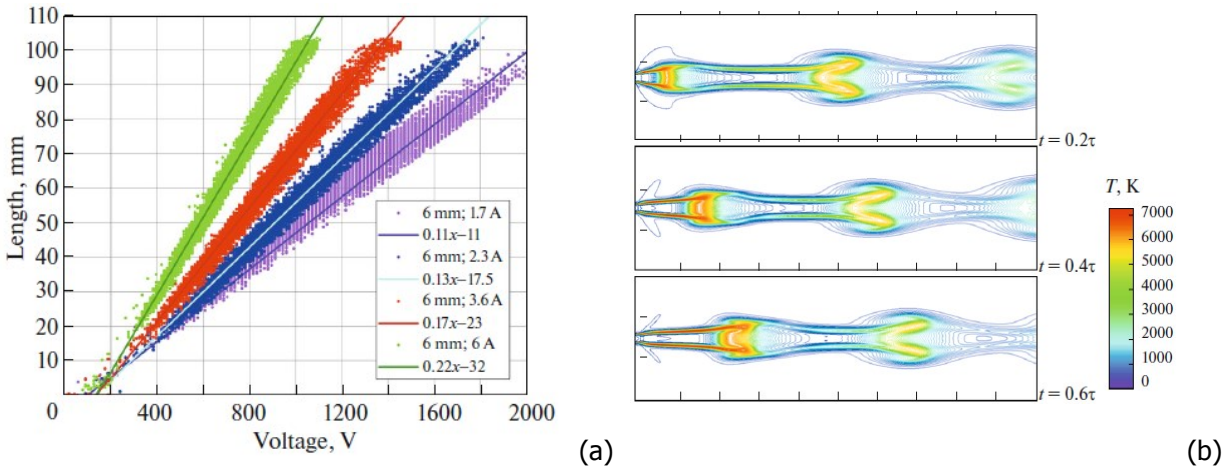

Fig 2. Dependences of the discharge length on its voltage at different currents (a) [10]. Temperature during one period between re-breakdowns for a current of 500 A/m. τ ~100 μs. Area dimensions: 200×60 mm. [13]

2.2. Longitudinal DC-discharge

The configuration of the longitudinal discharge has been studied in detail both experimentally and numerically [12]. For numerical modeling, this formulation of the problem is convenient because it allows one to perform calculations using 2D code in an axisymmetric sector formulation. The simulation was performed in the Plasmaero software package, taking into account plasma chemistry (with 11 components (N_2, O_2, NO, N, O, N_2+, O_2+, NO+, N+, O+, e) and 97 thermochemical reactions, supplemented by 5 reactions involving electrons in strong electric fields) [12], and in the FlowVision software using the air model from the work of M.Capitelly [17]. Some FlowVision simulation results are presented in Fig. 3. As a result of experiments and simulations, the voltage-current dependency was obtained (Fig.4a), as well as the dependence of plasma temperature on current. In the experiment, the temperature was obtained by analyzing the emission spectra of the second positive nitrogen system N_2(2+) [18]. It is shown that the discharge temperature increases rapidly with current increasing up to 1A (up to T = 5500 K), and after that the temperature growth rate decreases significantly - an increase in current to 7 A leads to an increase in temperature to 7000 K. This is primarily due to the dissociation of molecular nitrogen N_2. On the other hand, it was shown that an increase in current more than 3 A does not lead to a significant increase in the concentration of atomic oxygen produced in the discharge (Fig. 4b). And atomic oxygen has a significant effect on reducing the induction time at gaseous hydrocarbon fuel ignition [15].

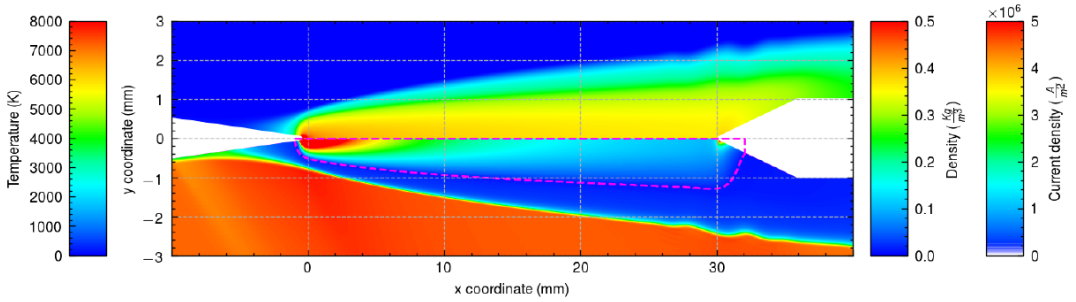

Fig 3. The results of numerical modelling of DC-discharge in a supersonic flow in FlowVision software package [12]

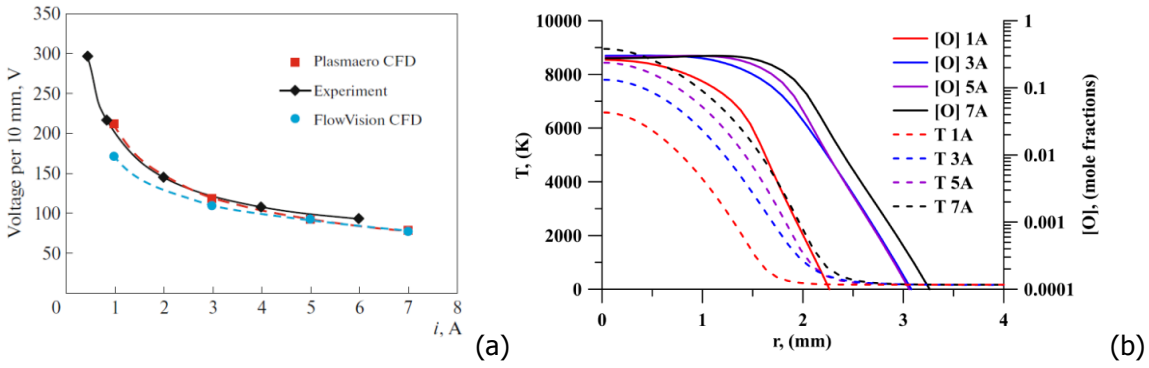

Fig 4. Voltage-current dependency of the discharge [18] (a). Radial distributions of O-atoms and temperature behind the discharge for current 5 A, calculated using Plasmaero [12] (b)

3. Study of ignition of a jet of air-fuel mixture in a supersonic flow

For a detailed study of the efficiency of ignition and flameholding in a supersonic flow using gas discharge plasma, we attempted to exclude the mixing factor of the injected fuel (ethylene) and the external supersonic air flow. Therefore, ethylene was pre-mixed with purified air (oxidizer) in a specially designed gas mixing system. It was designed for operating with stoichiometric ratio and with the possibility of deviating from it. The air flow rate was selected so that the pressure in the jet at the nozzle outlet was close to the pressure of the incoming supersonic flow.

3.1. Preliminary results of numerical simulation of plasma-stimulated combustion in a supersonic flow

Combustion simulation of a supersonic air-fuel mixture jet in the presence of an electrical discharge was carried out using the FlowVision package using the URANS model with the k-Ɛ turbulence model under conditions similar to the planned experiment. The plasma model and the electrodynamic model used were the same as in the authors' previous work on modeling a longitudinal discharge [12]. The calculation was carried out in a two-dimensional axisymmetric formulation. A cylinder sector with dimensions of 80 mm x 40 mm and an opening angle of 3.6 degrees was chosen as the computational domain geometry. Exit from the domain was free supersonic. A symmetry condition was set on the side walls of the sector, ensuring a zero gradient of physical quantities normal to the boundary. As a boundary condition for the entrance, a supersonic inlet was used with a specified temperature, velocity distribution, static pressure and concentrations of substances in the fuel-air mixture. At the inlet, P_{st} = 22 kPa, M = 2, T_g = 170 K were set, the ratio of the methane mass fraction to the air mass fraction was 1:17 within 4 mm from the axis of symmetry.

The discharge was directed along the flow and was located in its core at the axis. The electrodes are cylindrical with conical ends with a diameter of 1 mm and 2 mm. A boundary condition with constant electric current of 1 A was set on the front electrode. The second electrode had a constant potential of 0 V. The initial conditions in the entire volume corresponded to the boundary condition at the inlet, and the computational domain was filled with air. The initial conducting channel was established by setting the high enough temperature in a thin cylinder connecting the electrodes. Methane combustion was simulated using a simplified scheme of chemical reactions from the work [19], where it is designated as JL2. It consists of two direct and two reversible reactions and is an actual modification of the well-known Jones–Lindstedt combustion mechanism. The scheme was previously verified using 0D and 1D tests in FlowVision and Cantera, as well as a 2D simulation of a Bunsen burner was also performed. Testing of a similar scheme for ethylene is still in progress. Such modeling, which combines combustion and an electrodynamic model that takes into account the movement of the discharge channel in the volume, has significant novelty. In most known studies, the discharge is simulated using a volumetric heat source with static shape.

The results obtained indicate that despite the high discharge temperature (more than 5000 K), only partial conversion occurs, a significant amount of hydrogen and oxygen remains in the discharge zone (Fig. 5, Fig. 6), and a gradual conversion of CO to CO_2 also occurs. It is also clearly seen that the front of chemical reactions does not propagate against the flow and moves slightly across the flow from the high temperature region around the discharge. Numerical studies in this setting are ongoing.

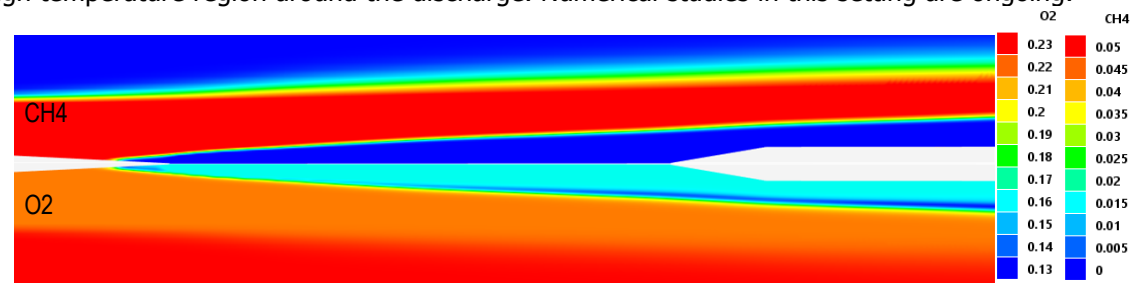

Fig 5. Distribution of mass fraction of methane and mass fraction of oxygen

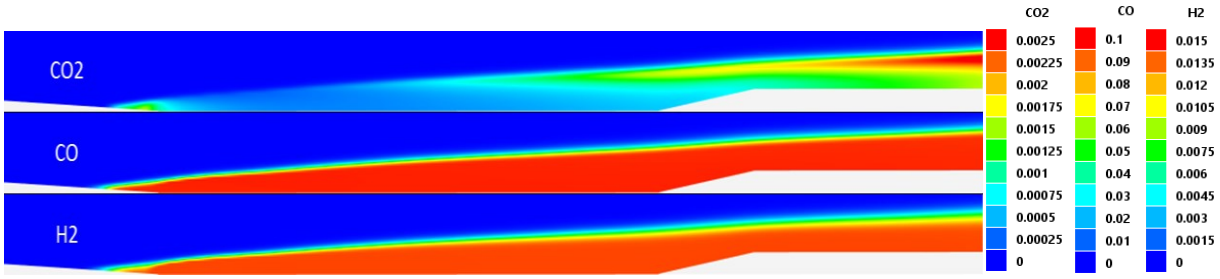

Fig 6. Distribution of mass fractions of carbon dioxide, carbon monoxide and hydrogen

3.2. Preparation of the experiment and description of the experimental configuration

The experiments were performed in the pulsed supersonic wind tunnel IADT-50 in JIHT RAS. The scheme of the test section is shown in Fig. 7. The test section of the tunnel has the cross-section size 60x70mm with expansion to 70x70 mm in the center, and is 600 mm long. A pylon with a height of 26mm was installed. In this configuration, a streamlined profiled pylon was used for injection of a pre-mixed fuel-air mixture. The pylon consists of two parts: a thin streamlined base 6mm thick and a Laval nozzle with an inner diameter at the outlet of 8mm and an outer diameter of 10mm. The Laval nozzle is necessary for the injected mixture parameters to match the external flow parameters: M = 2, V~500 m/s, T_g = 170 K, P_{st} = 22 kPa. The geometry of the pylon allows for minimizing the influence of the pylon elements on the combustion region in the supersonic flow. A DC discharge was ignited in the flow core downstream of the pylon. It had a longitudinal axisymmetric configuration, similar to the discharge in [12]. Power was supplied from a 5 kV DC source through ballast resistance R_1, which regulated the mean discharge current in the range of 4-7.5A. The resistance in the ignition circuit R_2 was 2 kOhm. The electrode connection scheme is shown in Fig. 7.

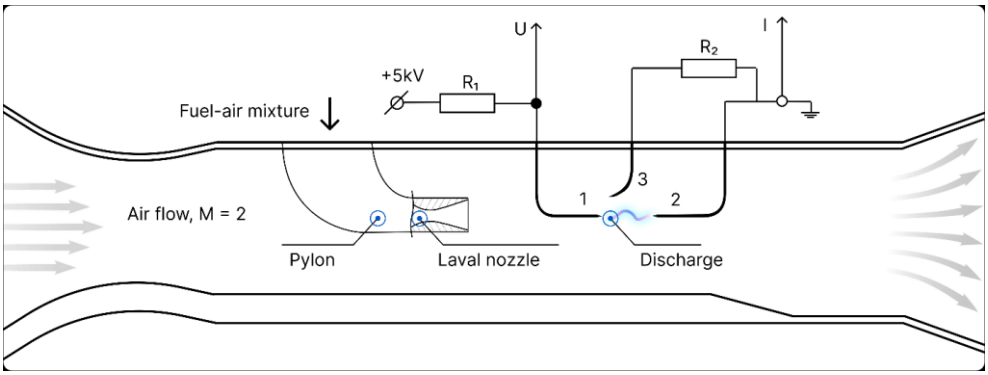

Fig 7. Scheme of the test section of the experiment

During the experiments, high-speed imaging of the combustion region was performed using a Photron S9 camera with a shutter speed of 1-2 μs; the flow structure was recorded using a high-resolution Schlieren system with a shutter speed of 100 ns (the exposure is determined by the duration of the laser-pulse illumination). Oscillograms of discharge current and voltage were obtained using a Tektronix DPO7054 multichannel digital oscilloscope with bandwidth up to 25 MHz. The ethylene flow rate was strictly controlled and recorded using an Alicat scientific flow meter with a 1ms sampling rate. The static pressure of the mixture before pylon air was obtained using a Honeywell pressure transducer with <1ms sampling frequency, and the required flow rate of air in the injected jet was controlled from the transducer data. The static pressure distribution along the test section was obtained using a pressure scanner with sensors installed on the wall of the test section.

During the preparation for the experiments, a preliminary numerical simulation of this setup was performed. Using multidisciplinary software package FlowVision the flow around the pylon was calculated, as well as the flow inside the pylon and a special section preceding the pylon, in which air was mixed with ethylene. The method of unsteady Reynolds-averaged Navier-Stokes equations was used with one of the standard FlowVision turbulence models based on the k-ε model.

The geometry in the computer model corresponds to a section of the wind tunnel with the pylon and a curved path for supplying the fuel-air mixture. The inlet flow parameters corresponded to the operating conditions of the supersonic wind tunnel: M = 2, T_g = 170 K, P_{st} = 22 kPa. Mass flow rates were set as boundary conditions responsible for the air and ethylene inlet into the mixer: for ethylene 1 g/s; for air - 17 g/s. As can be seen in Fig.8, the used variant of the mixer allows obtaining a well-mixed jet. The developed pylon has a sufficiently well streamlined shape which keeps the flow supersonic in the wake of the pylon in almost entire cross section of the wind tunnel. The nozzle of the pylon forms a long supersonic jet of the fuel-air mixture. Nevertheless, the pylon causes a complex structure of oblique shocks, which may cause difficulties in interpreting the data obtained from the pressure sensors.

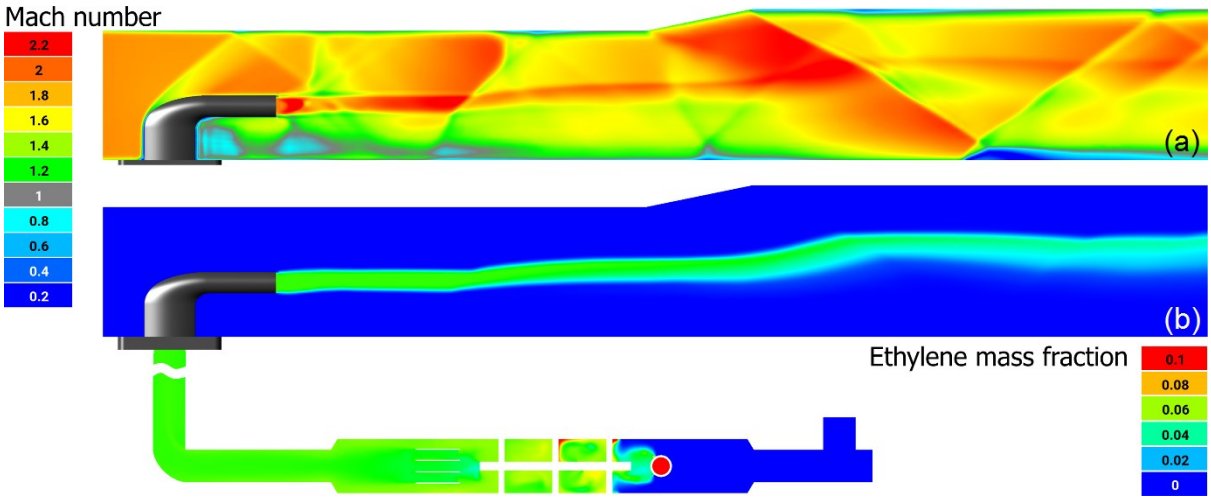

Fig 8. Mach number (a) and ethylene mass fraction (b) in the symmetry plane

3.3. Experimental results and discussion

A series of experiments was performed in which a pre-mixed fuel-air mixture was injected into the core of a supersonic air flow. The mass flow rate of ethylene was controlled by means of the pressure in an ethylene tank and the needle valve. It was set in range from 0.5 to 3 g/s. The air flow rate was unified for all experiments. The air flow was 17 g/s according to the analysis of the static pressure data. Then, after the flow rate and pressure had stabilized (the flow in the pylon has reached a supersonic mode), a discharge was ignited between the front (1) and initiating (3) electrode. The formed loop was carried downward by the flow and the current channel was reconnected to the downstream electrode (2) and the discharge operates in the longitudinal mode. The current in the experiments was 4-7.5 A, the voltage was 550-700 V, and the energy input varied from 2.6 kW to 4.1 kW.

Schlieren imaging allows visualizing the density gradients of the medium. In this experiment, a cone of heated gas is formed under the influence of a DC discharge. A typical obtained image of a supersonic flow during the experiment with combustion is shown in Fig. 9a. From the obtained frames, the thickness of the heat cone was determined using the image editor. It was obtained that in the absence of ethylene in the jet injected through the pylon, the thickness of the thermal cone behind the electrodes was about 13 mm, but with the ethylene mass flow rate of 2.9 g/s the average thickness of the thermal cone was 19 mm.

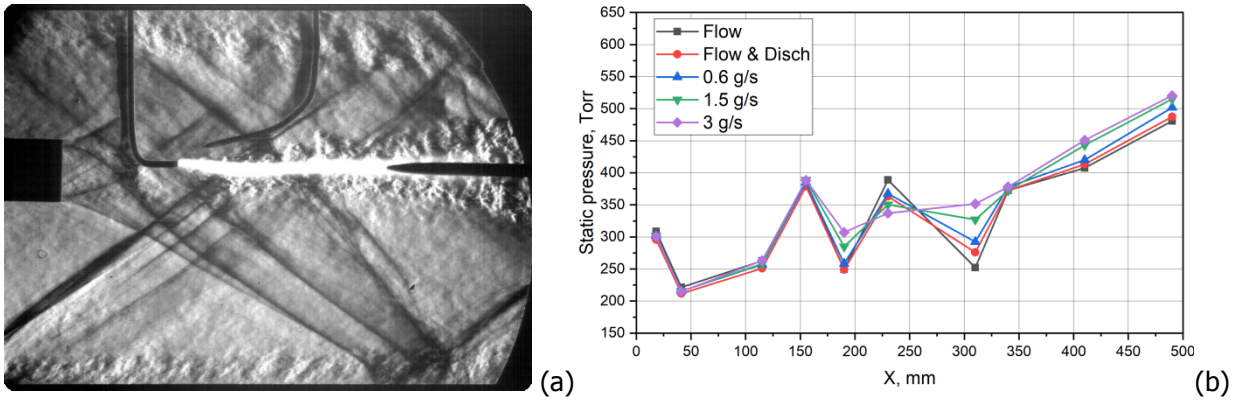

Fig 9. Typical schlieren image obtained in a combustion experiment (a); static pressure distribution on the wall of the test section for a given configuration (b)

In addition to Schlieren visualization, the pressure scanner allows to identify the ignition process of the fuel-air mixture in the flow. A total of 10 pressure sensors are installed on the wall of the test section. The coordinates of the pressure sensors are counted from the beginning of the insertion with the pylon and electrodes into the channel, the nozzle end of the pylon is located at a distance of 80 mm from the beginning of the insertion. As shown in Fig. 9b, in the absence of ethylene, and hence of ignition, the pressure at the wall did not change from discharge activation. On the contrary, when the fuel was fed

with mass flow rate of 2.9 g/s at a discharge current of 7.5 A, the pressure increased in the sensors starting from 150 mm and at some points the pressure increase reached 100 Torr relative to the case without discharge. This may indicate that partial oxidation of ethylene occurs in the flow downstream of the electrodes.

However, as can be seen from Fig. 9b, in this configuration the fuel-air mixture shows a worser combustion characteristics compared to the data presented in [4]. We assumed that this difference is conditioned by the lower energy input to the discharge due to the low discharge length. Therefore, it was decided to change the electrode configuration. In the new configuration, the 3rd electrode is taken out of the channel, the 2nd electrode is grounded, and the discharge is ignited and operates between the 1st and initiating electrode in the shape of a loop. I.e., a longitudinal-transverse discharge configuration is realized. In this geometry, the power can reach up to 10kW, while the average value is 6 kW (without taking into account that only 50 percent of the plasma filament is located in the zone of the jet, hence only half of the energy input is transferred to the ignited mixture). The re-breakdown frequency of the discharge in the updated configuration was estimated to be about 3.5 kHz. Schlieren visualizations of the longitudinal-transverse discharge for the cases in which the discharge was initialized in the absence and presence of ethylene (mass flow rate - 2.9 g/s) are demonstrated in Fig. 10. It shows that the thermal cone in the case with combustion became wider and corresponds to 18 mm, in contrast to the case with a discharge without ethylene in the jet, in which the cone width was only 11 mm.

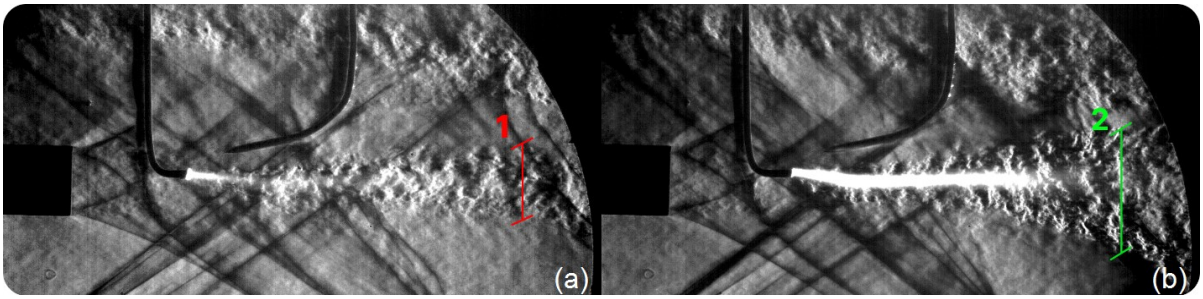

Fig 10. Comparison of images for discharge with current 7.5A for updated configuration of electrodes: a - without fuel, b - with fuel (2.9 g/s); thickness of the thermal cone at a distance of 50 mm from the tip of the front electrode: 1–11 mm, 2–18 mm

The distribution of static pressure on the top wall of the test section for the updated configuration was obtained. The graph of pressure dependence on the x-coordinate of the wind tunnel test section is presented in Fig. 11. The ignited discharge without fuel supply does not affect the pressure distribution in the test section. However, when fuel is supplied during the discharge operation, the pressure increases near the wall. At some points the pressure increases by 400 torr due to combustion. With increasing of the ethylene mass flow rate in the experiment, the static pressure at the wall increases.

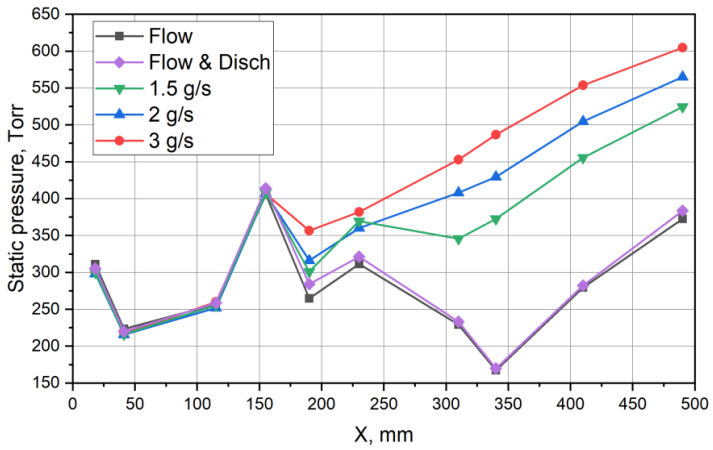

Fig 11. Static pressure distribution along the upper wall of the test section for a longitudinal-transverse discharge at a current of 7.5 A

4. Conclusion

Experimental and numerical studies of direct current discharge (longitudinal and longitudinal-transverse) in a supersonic flow were performed. Properties of the discharge were obtained: the dependence of the discharge temperature on the current, the current-voltage characteristic and other. The results of modeling a discharge in a supersonic flow in the CFD software Plasmaero and FlowVision are in good agreement with the experimental data. Based on previous results and the properties of discharge, new experiments on plasma-assisted combustion were performed. In these experiments the fuel was pre-mixed with air, supplied in the supersonic mode to the core of a supersonic flow and ignited by the discharge. This formulation of the problem excludes the influence of mixing and subsonic separation zones on the result of the experiment. It is shown that, despite preliminary mixing, an elongated powerful plasma channel is required for ignition. Therefore, influence of mixing looks to be lower than length and power of the discharge. At the same time, experiments performed demonstrates that it is possible to ignite and stabilize the flame front even in the case of supersonic motion of flow and mixture at the absence of separation zone.

Acknowledgements

The work was supported by the Russian Science Foundation grant No. 21-79-10408.

References

1. Caruana, D.: Plasmas for Aerodynamic Control. *Plasma Phys Control Fusion* **(2010)**. https://doi.org/10.1088/0741-3335/52/12/124045
2. Firsov, A.A., Savelkin, K.V., Yarantsev, D.A., Leonov, S.B.: Plasma-Enhanced Mixing and Flameholding in Supersonic Flow. *Philos. Trans. R. Soc.* **(2015)**. https//doi.org/10.1098/rsta.2014.0337
3. Leonov, S.: Electrically Driven Supersonic Combustion. *Energies (Basel)* **(2018)**. https://doi.org/10.3390/en11071733
4. Firsov, A.A.: Experimental Investigation of Flameholding in Scramjet Combustor by Pylon with Plasma Actuator Based on Q-DC Discharge. *Aerospace* **(2023**). https://doi.org/10.3390/aerospace10030204
5. Leonov, S.B., Elliott, S., Carter, C., Houpt, A., Lax, P., Ombrello, T.: Modes of Plasma-Stabilized Combustion in Cavity-Based M = 2 Configuration. *Exp Therm Fluid Sci* **(2021)**. https://doi.org/10.1016/J.EXPTHERMFLUSCI.2021.110355
6. Feng, R., Zhu, J., Li, D., Meng, Z., Sun, M., Wang, H., Wang, C., Wang, C., Wang, Z.: Characteristics of the Flame Flashback in a Dual-Mode Scramjet Combustor by the Gliding Arc Plasma. *Applications in Energy and Combustion Science* **(2023)**. https://doi.org/10.1016/j.jaecs.2023.100143
7. Houpt, A., Brock, H., Leonov, S., Ombrello, T., Campbell, Carter.: Quasi-DC Electrical Discharge Characterization in a Supersonic Flow. *Exp Fluids* **(2017)**. https://doi.org/10.1007/s00348-016-2295-5
8. Efimov, A.V., Firsov, A.A., Kolosov, N.S., Leonov, S.B.: Characterization of Electric Discharge Collocated with Gas Jet in Supersonic Airflow. *Plasma Sources Sci Technol* **(2020)**. https://doi.org/10.1088/1361-6595/AB9C94
9. Logunov, A.A., Kornev, K.N., Shibkova, L.V., Shibkov, V.M.: Influence of the Interelectrode Gap on the Main Characteristics of a Pulsating Transverse-Longitudinal Discharge in High-Velocity Multicomponent Gas Flows. *High Temperature* **(2021)**. https://doi.org/10.1134/S0018151X21010119
10. Perevoshchikov, E.E., Firsov, A.A.: Influence of Current and Interelectrode Gap on Characteristics of Longitudinal-Transverse Discharge in a Supersonic Airflow. *Plasma Physics Reports* **(2023)**. https://doi.org/10.1134/S1063780X22601894

11. Kornev, K.N., Logunov, A.A., Shibkov, V.M.: Simulation of a Transverse–Longitudinal Discharge in a Supersonic Air Flow in the Hydrodynamic Approximation. *Plasma Physics Reports* **(2023)**. https://doi.org/10.1134/S1063780X22602139

12. Firsov, A., Bityurin, V., Tarasov, D., Dobrovolskaya, A., Troshkin, R., Bocharov, A.: Longitudinal DC Discharge in a Supersonic Flow: Numerical Simulation and Experiment. *Energies (Basel)* **(2022)**. https://doi.org/10.3390/en15197015

13. Bityurin, V.A., Bocharov, A.N., Dobrovolskaya, A.S., Popov, N.A., Firsov, A.A.: Re-Breakdown Process at Longitudinal-Transverse Discharge in a Supersonic Airflow. *Plasma Physics Reports* **(2023)**. https://doi.org/10.1134/S1063780X22601869

14. Bourlet, A., Labaune, J., Tholin, F., Pechereau, F., Vincent-Randonnier, A., Laux, C.O.: Numerical Model of Restrikes in DC Gliding Arc Discharges. *AIAA SciTech Forum* **(2022).** https://doi.org/10.2514/6.2022-0831

15. Bityurin, V.A., Dobrovolskaya, A.S., Bocharov, A.N., Firsov, A.A.: Atomic Oxygen Generation by Longitudinal-Transverse Discharge. *Plasma Physics Reports* **(2023).** https://doi.org/10.1134/S1063780X22601857

16. Tarasov, D.A., Firsov, A.A. CFD Simulation of DC-Discharge in Airflow.: *J Phys Conf Ser* **(2021)**. https://doi.org/10.1088/1742-6596/2100/1/012015

17. D'Angola, A., Colonna, G., Gorse, C., Capitelli, M.: Thermodynamic and Transport Properties in Equilibrium Air Plasmas in a Wide Pressure and Temperature Range. *The European Physical Journal D* **(2007**). https://doi.org/10.1140/EPJD/E2007-00305-4

18. Troshkin, R.S., Firsov, A.A.: Parameters of a Longitudinal DC Discharge in a Supersonic Air Flow. *Plasma Physics Reports* **(2023)**. https://doi.org/10.1134/S1063780X22601870

19. Wang, L., Liu, Z., Chen, S., Zheng, C.: Comparison of Different Global Combustion Mechanisms Under Hot and Diluted Oxidation Conditions. *Combustion Science and Technology* **(2012)**. https://doi.org/10.1080/00102202.2011.635612